State of the art imaging in Meniere's disease. Tips and tricks for protocol and interpretation

Pont, L.M.H. de; Steekelenburg, J.M. van; Verbist, B.M.; Buchem, M.A. van; Blom, H.M.; Hammer, S.

State of the Art Imaging in Menière's Disease. Tips and Tricks for Protocol and Interpretation

Lisa M. H. de Pont[1,2] · Josephine M. van Steekelenburg[1] · Berit M. Verbist[2] ·
Mark A. van Buchem[2] · Henk M. Blom[3] · Sebastiaan Hammer[1]

Abstract

Purpose of Review Menière's disease (MD) is a burdensome and not well understood inner ear disorder that has received increasing attention of scientists over the past decade. Until 2007, a certain diagnosis of endolymphatic hydrops (EH) required post-mortem histology. Today, dedicated high-resolution magnetic resonance imaging (MRI) protocols enable detection of disease-related changes in the membranous labyrinth in vivo. In this review, we summarize the current status of MR imaging for MD.
Recent Findings The mainstays of hydrops imaging are inversion recovery sequences using delayed acquisition after intravenous or intratympanic contrast administration. Based on these techniques, several methods have been developed to detect and classify EH. In addition, novel imaging features of MD, such as blood-labyrinth barrier impairment, have recently been observed.
Summary Delayed contrast enhanced MRI has emerged as a reliable technique to demonstrate EH in vivo, with promising application in the diagnosis and follow-up of MD patients. Therefore, familiarity with current techniques and diagnostic imaging criteria is increasingly important.

This article is part of the Topical Collection on *ENT Imaging*.

✉ Lisa M. H. de Pont
l.depont@hagaziekenhuis.nl

1 Department of Radiology, Haga Teaching Hospital, Els-Borst Eilersplein 275, 2545 AA The Hague, The Netherlands

2 Department of Radiology, Leiden University Medical Center, Albinusdreef 2, 2333 ZA Leiden, The Netherlands

3 Department of Otorhinolaryngology, Haga Teaching Hospital, The Hague, The Netherlands

Introduction

Menière's disease (MD) is a clinical condition defined by spontaneous episodes of vertigo associated with low frequency sensorineural hearing loss, tinnitus and/or aural pressure [1]. It affects approximately 17–513 per 100,000 adults with a peak incidence in the 40–50 years age group [2]. The condition is named after the French neurologist Prosper Menière, who identified the inner ear as the site of origin in 1861 as opposed to the central nervous system as previously believed [3, 4]. MD usually presents with unilateral symptoms, but the development of bilateral clinical disease is frequent as it has been reported in up to 78% of cases [5]. Endolymphatic hydrops (EH), a distention of the endolymphatic compartments of the inner ear into the surrounding perilymphatic space, is considered the pathological hallmark of MD since it was first reported by Hallpike and Yamakawa on temporal bone examinations in 1938 [6, 7]. A schematic drawing of the labyrinthine structures is shown in Fig. 1a. EH can affect the cochlear duct and saccule, but may also involve the utricle, ampullae and semicircular ducts [8]. Although many theories have been proposed, the etiology of EH remains unknown and the relationship between EH and the clinical manifestations of MD have not been clarified [•9].

The diagnostic guidelines as provided by the American Academy of Otolaryngology-Head and Neck Surgery (AAO-HNS), which were originally published in 1972 and subsequently revised in 1985 and 1995, have greatly aided the identification of patients suffering from MD from a clinical standpoint [10]. In 2015, the Classification

Committee of the Bárány Society proposed a new consensus document with diagnostic criteria for MD, which were reviewed by the Equilibrium Committee of the AAO-HNS and subsequently approved as an amendment to the 1995 guidelines. The 2015 criteria recognize two probabilistic categories of the condition: *definite MD* and *probable MD* (Table 1) [•11, 12]. However, diagnosis remains challenging in patients that do not present with the typical symptom triad. Moreover, MD constitutes a chronic and progressive disease in which it may take up to 10 years for the full clinical picture to develop [13]. Patients may therefore present with non-specific symptoms that demonstrate a high degree of overlap with other vertigo-associated diseases, which complicates the process of diagnosis. Numerous tests for the indirect demonstration of EH, such as electrocochleography (ECoG), caloric testing, and vestibular-evoked myogenic potentials (VEMP), have been developed; however, no specific test for MD exists [2]. One of the greatest advancements concerning the diagnosis of MD is the visualization of EH in living MD patients using magnetic resonance imaging (MRI) with delayed acquisition after intratympanic administration of gadolinium-based contrast media (GBCM) in 2007 [14]. In 2010, it was reported that EH can also be visualized after intravenous GBCM administration [15]. The endolymphatic and perilymphatic compartments can be distinguished by allowing dilute GBCM to accumulate within the perilymphatic space, thereby outlining the less permeable endolymphatic space. This allows for the demonstration of EH [14, 15]. The amount of research that has since been devoted to MD has considerably increased and many studies have demonstrated the feasibility of these techniques. Further advances have led to the development of various imaging sequences and interpretation methods, which are increasingly applied in clinical practice [16–18].

The purpose of this article is to review the current state-of-the-art MRI techniques for suspected MD. The most commonly used MRI sequences to evaluate the inner ear compartments, including technical and practical considerations, are described. Next, contemporary grading methods for EH and novel MRI features that have arisen in the recent literature are reviewed. Finally, clinical utility and describe future perspectives are discussed.

Visualization of Endolymphatic Hydrops

The concept of hydrops imaging relies on the selective enhancement of perilymphatic fluid using delayed MRI acquisition after administration of GBCM [16].

Administration of Gadolinium-Based Contrast Media

EH can be visualized on MRI after intratympanic (IT) or intravenous (IV) GBCM administration [14, 15]. The IT method was first applied in animal studies, and subsequently adapted for the visualization of EH in humans at 3T (3T) MRI by Nakashima et al. in 2007 [14, 19, 20]. This method requires a puncture of the tympanic membrane and injection of 0.3–0.6 ml of eightfold diluted GBCM into the tympanic cavity [16]. Fivefold or 16-fold dilutions have also been reported [21, 22]. Following injection, GBCM diffuses from the tympanic cavity across the round window membrane and distributes throughout the perilymphatic space [16]. For the IT method, MRI acquisition is typically performed 24 h after injection [14]. In 2010, further developments by Nakashima et al. led to the first demonstration of EH at 3T MRI after IV contrast administration [15]. These authors used a double dose of GBCM. However, other researchers have managed to detect EH after a single dose of IV GBCM and the ideal dose of contrast is currently under debate [23, ••24, 25].

Previous studies investigating optimal timing of MRI acquisition after IV GBCM administration have demonstrated peak enhancement of the perilymph after 3.5 to 4.5 h and plateauing of the endolymphatic volume after 4.5 to 6 h [26–28]. Most clinical studies wait 4 h after IV GBCM administration, which effectively results in a time delay of 4.5 h including patient set-up, localizing scan and acquisition time [••29, ••30, 31, 32]. Notably, it was recently reported that the degree of EH may be overestimated on images obtained within 1.5 h due to insufficient accumulation of GBCM in the perilymph fluid, thereby underlining the necessity of adequate timing in clinical practice [28].

IT and IV GBCM administration in MD patients each have pros and cons, as has been discussed in detail by Naganawa et al. [16]. In short, IT administration has the advantage of achieving better perilymph-endolymph contrast compared to IV administration due to higher local GBCM concentrations, especially in the basal cochlear turn [16, 33]. However, this method is considered off-label use of GBCM, requires a longer waiting time before MRI acquisition, and the signal intensity of the perilymph depends on the permeability of the round window membrane which can be impaired in some patients [16]. In addition, this method may potentially cause local irritation and toxicity, though previous studies investigating hearing function after IT GBCM administration have revealed no short- or long-term ototoxicity [17, 34–36]. The intravenous route is less invasive, results in more homogenously distributed GBCM, and offers the possibility of evaluating both ears simultaneously, which is relevant in the assessment of bilateral disease [16, •37]. Both the IV
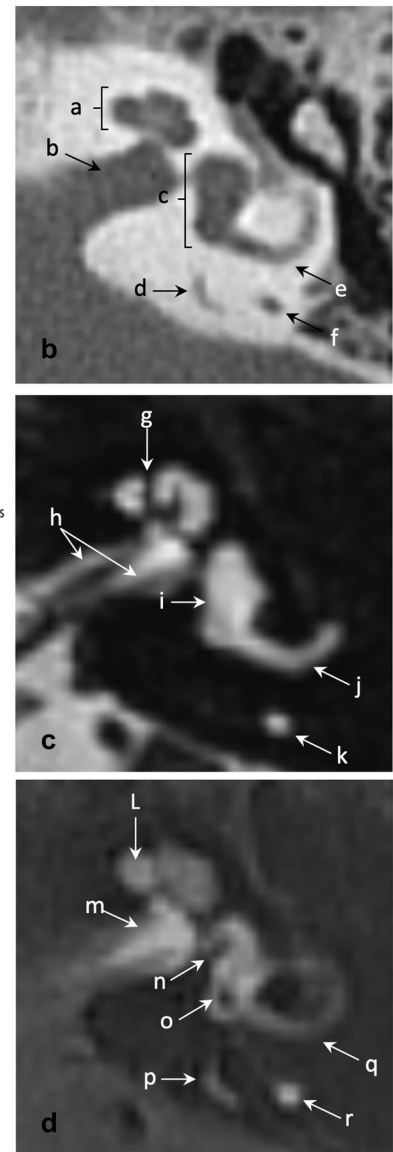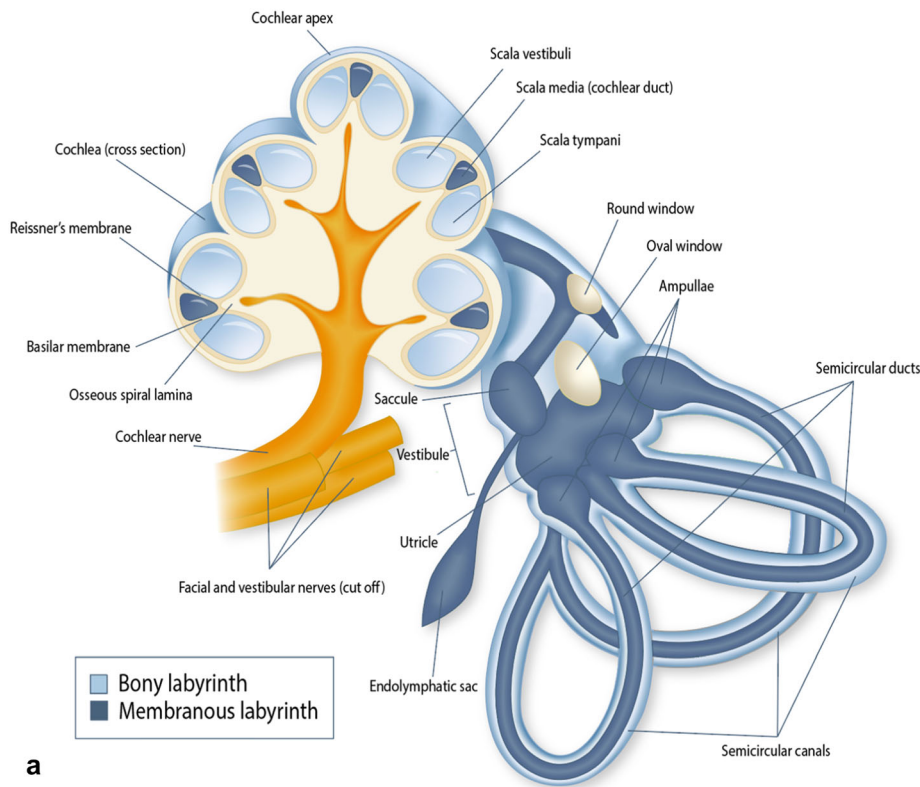
Fig. 1 Anatomy of the inner ear. **a** Schematic depiction of the inner ear, which is composed of a bony and membranous labyrinth. The bony labyrinth consists of a collection of perilymph-filled cavities in the petrous temporal bone: the cochlea, vestibule and semicircular canals. Within the bony labyrinth lies the membranous labyrinth, which is filled with endolymph. In the cochlea, the membranous labyrinth is composed of the scala media (also called the cochlear duct), which contains the sensory organ for hearing. At the base, the scala media is separated from the scala tympani by the basilar membrane and osseous spiral lamina. The roof of the scala media is formed by Reissner's membrane, which distends into the scala vestibuli in case of endolymphatic hydrops. The membranous labyrinth in the vestibule consists of two endolymphatic structures: the saccule and utricle. The saccule, usually the smallest of the two vestibular sacs, lies in the pars inferior of the vestibule whereas the utricle lies in the pars superior. The endolymphatic duct (ED) leads from the posteromedial surface of the vestibule through the osseous vestibular aqueduct (VA) to the endolymphatic sac (ES). The latter located partly within the VA and partly within the dura of the posterior fossa. The semicircular canals enclose three membranous semicircular ducts (horizontal, posterior, superior), which open into the utricle by expanded ends called ampullae. The saccule, utricle and semicircular ducts are dedicated to the perception of balance and equilibrium. **b** Axial CT of the left petrous temporal bone demonstrating the bony labyrinth. *A = cochlea; b = internal auditory canal; c = vestibule; d = vestibular aqueduct; e = horizontal semicircular canal; f = posterior semicircular canal.* **c** Axial T2 SPACE MRI centered at the inferior vestibule, demonstrating the entire labyrinthine fluid space (endolymph and perilymph). *G = interscalar septum; h = cochlear and vestibular nerves; i = vestibule; j = horizontal semicircular canal; k = posterior semicircular canal.* **d** Normal morphology of the membranous labyrinth on 4 h-delayed Gd-enhanced 3D-FLAIR MRI, centered at the inferior vestibule. The hypointense endolymphatic spaces of the cochlea and vestibule are surrounded by hyperintense perilymph. Note that the membranous ED and ES appear hyperintense, presumably due to a surrounding vascular network as they do not contain a surrounding perilymphatic space. *L = barely perceptible hypointense scala media/osseous spiral lamina; m = physiological enhancement of the fundus of the internal auditory canal; n = saccule; o = utricle; p = endolymphatic duct and sac; q = horizontal semicircular duct; r = posterior semicircular canal*

Table 1 Diagnostic criteria for Menière's disease

1995 AAO-HNS diagnostic guidelines [10]	
Certain MD	Definite Menière's disease, plus histopathologic confirmation of hydrops
Definite MD	Two or more definite spontaneous episodes of vertigo 10 min or longer
	Audiometrically documented hearing loss on at least 1 occasion
	Tinnitus or aural fullness in the treated ear
	Other causes excluded
Probable MD	One definite episode of vertigo
	Audiometrically documented hearing loss on at least 1 occasion
	Tinnitus or aural fullness in the treated ear
	Other causes excluded
Possible MD	Episodic vertigo of the Menière's type without documented hearing loss or sensorineural hearing loss, fluctuating or fixed, with disequilibrium but without definite episodes
	Other causes excluded
2015 Equilibrium Committee amendment to the 1995 AAO-HNS guidelines [•11, 12]	
Definite MD	Two or more spontaneous episodes of vertigo, each lasting 20 min to 12 h
	Audiometrically documented low- to midfrequency sensorineural hearing loss in 1 ear, defining the affected ear on at least 1 occasion before, during, or after 1 of the episodes of vertigo
	Fluctuating aural symptoms (hearing, tinnitus, or fullness) in the affected ear
	Not better accounted for by another vestibular diagnosis
Probable MD	Two or more episodes of vertigo, each lasting 20 min to 24 h
	Fluctuating aural symptoms (hearing, tinnitus, or fullness) in the affected ear
	Not better accounted for by another vestibular diagnosis

and IT method effectively result in accumulation of GBCM throughout the perilymphatic space, but not the endolymphatic space, thereby enabling the visualization of EH in patients with MD [16].

Several contrast agents have been used to visualize EH, including gadoterate megluminate (Dotarem®), gadobutrol (Gadovist®), gadodiamide (Omniscan®), and gadopentate gimeglumine (Magnevist®) [14, 22, ••24,•• 29, 32, 38, 39]. The contrast effect in symptomatic ears of MD patients was reported to be comparable between eightfold diluted gadopentate gimeglumine and gadodiamide for the IT method, and between gadoterate megluminate and gadobutrol for the IV method respectively [40, 41]. However, the perilymph signal intensity in the contralateral asymptomatic ear was reported to be higher with IV gadobutrol than IV gadoterate megluminate, which benefits assessment of silent (subclinical) EH [41]. The difference in the degree of T1 shortening of the gadolinium(Gd)-enhanced perilymph between these two contrast agents has not been fully clarified, but is likely due to the greater longitudinal relaxivity of gadobutrol [41, 42]. This finding may be relevant with regard to future development of low-dose Gd-enhanced MRI protocols for hydrops imaging.

Hydrops Sequences

The most commonly used sequences for hydrops imaging are three-dimensional fluid-attenuated inversion recovery (3D-FLAIR) and three-dimensional real inversion recovery (3D-real IR), currently mainly performed at 3T [16]. Both techniques rely on inversion recovery (IR) pulse sequences, but with different methods of image reconstruction: magnitude reconstruction and phase-corrected ("real") reconstruction respectively [43, 44]. 3D-FLAIR allows selective nulling of the endolymphatic space by selecting an inversion time (TI) such that at equilibrium there is no net transverse magnetization of endolymph [43]. This technique produces an image at which hypointense endolymph can be differentiated from hyperintense (Gd-enhanced) perilymph, but not from surrounding bone, which shows a signal intensity similar to endolymph on this sequence [43, 45]. This sequence is particularly sensitive to low concentrations of GBCM and therefore preferably used for hydrops imaging after IV GBCM administration [43]. Alternatively, the 3D-real IR sequence can be used to separate endolymph from perilymph and the surrounding bone by selecting a TI between the null point of endolymph and Gd-enhanced perilymph [44, 46]. This technique is

predominantly used after IT GBCM administration in which local contrast concentrations are higher compared with the IV method [16]. However, due to the invasiveness of IT contrast administration, the 3D-FLAIR sequence after IV GBMC has become increasingly popular [18]. Parameters for the 3D-FLAIR sequence may vary and are summarized in Table 2. Generally, the TI ranges from 2000 to 2500 ms at 3T [•47]. It is of importance to realize that the TI applied for IR sequences may influence the endolymph-perilymph ratio: a longer TI generally provides better identification of the perilymph signal, whereas the endolymphatic spaces are generally better appreciated on images with short TI [•47–49].

Besides the conventional 3D-FLAIR or 3D-real IR sequences, alternative MRI analysis has been proposed through optimized heavily T2-weighted 3D-FLAIR sequences, the subtraction of two IR sequences with different inversion time, or subtraction of a balanced fast field echo (FFE) sequence from a 3D-FLAIR sequence [50–52]. The use of non-contrast MRI for MD has not been widely investigated. Saccular morphology was evaluated using a 3D T2-weighted steady state free precession (SSFP) sequence and 3D heavily T2-weighted constructive interference in steady state (CISS) sequence respectively [53, 54]. These techniques, however, do not allow identification of the utricle, ampullae or cochlear duct.

Table 2 Imaging protocols for delayed Gd-enhanced 3D-FLAIR MRI at 3T

	Attyé [••24]	Bernaerts [••30]	Dubrulle [80]	Gürkov [95]	van Steekelenburg [••29]
Year	2017	2019	2020	2011	2019
Intervention	Intravenous single dose Gadoterate meglumine (0.1 mmol/kg)	Intravenous gadobutrol (0.1 mmol/mL, 0.2 mmol/kg)	Intravenous single dose gadoterate meglumine (0.1 mmol/kg)	Intratympanic administration of 0.4 mL 1:8 diluted gadodiamide	Intravenous double dose (30 mL) gadoterate meglumine (0.5 mmol/mL)
Acquisition time delay	4 h	4 h	4–5 h	20–24 h	4 h
Coil	32-channel SENSE head coil	32-array head coil	32-channel SENSE head coil	12-channel coil	20-channel head coil
TR (ms)	7600	6000	8000	9000	6000
TE (ms)	345	168	316	128	177 / 182*
TI (ms)	2300	2000	2400	2500	2000
FS	n.a	n.a	SPAIR	n.a	n.a
Voxel size (mm)	0.8 × 0.8 × 0.8	0.5 × 0.5 × 0.8	0.8 × 0.8 × 0.8	0.4 × 0.4 × 2.0	0.5 × 0.5 × 0.8 / 0.6 × 0.6 × 0.6*
Flip angle	Variable flip angles using the Brainview® technique	180°	160° to 30°, then progressive return to initial angles	Constant flip angle echo train with flip angle of 180° for conventional turbo spin echo refocusing echo train	180°
NEX/NSA	2	1	2	1	1
Parallel acquisition, factor	SENSE, 4	GRAPPA, 2	SENSE, 2.5	GRAPPA, 2	GRAPPA, 2 / GRAPPA, 2.5*
FOV (mm)	Not reported	190 × 190	200 × 200	160 × 160	190 × 190 / 200 × 200*
Acquisition time	9 min	14 min	8 min 40 s	15 min	14 min / 12 min 2 s*

*The asterisk marks small adaptations in the previously published protocol (2020)

FOV field of view, *GBCM* gadolinium-based contrast media, *GRAPPA* generalized autocalibrating partially acquisition, *n.a* not applicable, *NEX* number of excitations, *NSA* number of signal averages/acquisitions, *SENSE* sensitivity encoding, *SPAIR* spectral attenuated inversion recovery, *TE* echo time, *TI* inversion time, *TR* repetition time

Considerations for MRI

MRI has predominantly been performed at 3T using a head coil with a high number of receiving channels to maximize signal-to-noise-ratio [•37]. Due to the small caliber of endolymphatic structures, a slice thickness of 0.8 mm or less is generally applied. Hydrops sequences are obtained in the axial plane parallel to the lateral semicircular canal, in accordance with current grading methods for EH, and are interpreted in conjunction with a 3D heavily T2-weighted sequence of the inner ear for reference of the total labyrinth fluid space [••29, •37]. Although isotropic data-sets are not required, multiplanar assessment has been advocated to avoid a false-positive diagnosis of EH [39]. Whole-brain sequences may be included if relevant. It is generally recommended to perform the MRI exam using a two-step approach: prior to GBCM administration, conventional inner ear and whole-brain sequences are obtained; then, 4 h after IV contrast injection (or 24 h after IT GBCM administration) the hydrops sequence is acquired. Alternatively, both conventional and hydrops sequences can be performed in one sitting 4 h after IV GBCM administration, although this eliminates the opportunity of obtaining nonenhanced images [•37]. Due to the time delay between contrast injection and imaging, logistical adjustments within the radiology department are required to ensure a smooth process. In addition to patient instruction, additional fixation can be placed between the patient's head and the receiver coil to further reduce motion artifacts [••29]. Scan times for the 3D-FLAIR sequence were initially rather long, up to 15 min, but have been reduced to 8–9 min by applying parallel imaging techniques and variable flip angles. However, 3D-FLAIR with a constant flip angle of 140° has recently been shown to yield a higher perilymph signal intensity ratio (SIR) than variable flip angle heavily T2-weighted 3D-FLAIR MRI [•55].

MRI Assessment

Normal MRI Findings

The radiologic morphology of the normal bony and membranous labyrinth is demonstrated in Fig. 1b, c and d. At delayed Gd-enhanced 3D-FLAIR MRI, the endolymphatic spaces appear as signal voids surrounded by hyperintense perilymph [56]. The saccule, normally the smallest of the two vestibular endolymphatic structures, is located inferior, medial and anterior in the vestibule [57]. The utricle is an elliptical structure located in the pars superior of the vestibule. In the axial plane, both saccule and utricle are generally best delineated at the inferior vestibule parallel to the horizontal semicircular canal. The cochlear duct is best evaluated at the mid-modiolar section, although barely perceptible due to its slim caliber and similar signal intensity as the osseous spiral lamina [45, 58]. Although the endolymphatic duct and sac contain endolymph fluid and are not surrounded by perilymphatic spaces, these structures appear hyperintense at delayed Gd-enhanced 3D-FLAIR MRI, which has been suggested to be due to enhancement of surrounding vascular structures [59].

Previous studies have described a physiological signal increase in several fluid-containing spaces other than the perilymphatic space on delayed Gd-enhanced MRI, such as the anterior eye chamber, Meckel's cave, the fundus of the internal auditory canal, and the subarachnoid space surrounding the optic nerves, which should not be mistaken for pathology [27, 60].

Diagnostic MRI Criteria

Since the first description of EH on MRI in MD patients, several qualitative and semi-quantitative methods have been proposed to classify the degree of EH for the cochlea and vestibulum separately [••24, ••29, ••30, 45, 56, 61, 62]. The first grading system proposed by Nakashima et al. defined vestibular hydrops as an endolymph-perilymph ratio of > 33%. For the cochlea, any visual bulging of the cochlear duct into the scala vestibuli—which indirectly demonstrates displacement of Reissner's membrane—was considered hydropic [45]. However, this classification was found to lack specificity and was subsequently modified into the 3-point scale by Baráth, which categorizes cochlear and vestibular hydrops as none, grade 1 or grade 2 [56]. The hydropic process often affects both the cochlea and vestibule, but vestibular hydrops has reported to be more prevalent at delayed Gd-enhanced MRI [13, ••29, 63, 64]. Paradoxically, a previous study investigating the distribution of EH from reports of 184 temporal bone specimens has described a cochleocentric distribution where hydrops predominates in the cochlea and from thereout progresses to involve the saccule, utricle, ampullae and semicircular ducts [8]. This discrepancy between radiological and histopathological studies has not yet been clarified, but may be explained based on differences between patient groups (living versus post-mortem) or the observation that low-grade EH is visually easier to diagnose in the vestibule than cochlea [65]. The saccule possesses the highest compliancy out of all the endolymphatic compartments, which would therefore seem most vulnerable to subtle changes in endolymphatic pressure [66]. In this light, Attyé et al. recently reported a low-grade distention of the saccule in MD patients. For the diagnosis of saccular EH, the utricle has been proposed as a reference

(i.e., saccule equal or larger than the utricle is considered pathological), with a sensitivity of 50% and a specificity of 100% for definite MD [••24]. An advantage of this method is that a saccule-utricle ratio is less dependent on the TI used for hydrops imaging, as opposed to the endolymph-perilymph ratio.

Increasing application of delayed Gd-enhanced MRI in patients with a variety of cochleovestibular symptoms has demonstrated that EH also occurs in patients with only one of the symptoms of the MD triad (vertigo, tinnitus or sensorineural hearing loss) [13]. In addition, EH has been observed in other inner ear lesions such as otosclerosis, endolymphatic sac tumor and vestibular schwannoma [67–69]. In this light, Gürkov et al. recently introduced the term "hydropic ear disease"—a paradigm shift from a symptom-based classification towards an imaging-based diagnosis [65]. This system divides inner ear diseases with EH on imaging into two categories: primary hydropic ear disease (PHED), i.e., EH without identifiable cause, and secondary hydropic ear disease (SHED), i.e., EH caused by underlying inner ear diseases [65, ••70]. This classification incorporates the full spectrum of symptoms in primary and secondary MD and allows recognition of atypical patients who do not fulfill the description of MD according to the current AAO-HNS criteria.

In addition to EH, multiple imaging studies have reported an increased post-contrast perilymph signal intensity in the affected ears of MD patients, which is believed to represent impairment of the blood-labyrinth barrier (BLB) [••29, ••30, 63, 71, 72]. This hypothesis is corroborated by histopathological studies in MD that demonstrated BLB dysfunction in the microvasculature of vestibular end organs in MD patients [73]. The observation of BLB impairment on MRI is, however, not exclusive for MD as similar findings have been reported in vestibular neuritis [74, 75], sudden sensorineural hearing loss [76] and vestibular schwannoma [77]. As such, increased peri-lymph signal intensity on its own is non-specific. However, the combination of EH and BLB impairment is highly specific for MD and, importantly, scarcely present in other vertigo-associated inner ear disorders with the exception of vestibular migraine [••29]. Lately, four-grade classifications have been proposed that take into consideration the

cochlear and vestibular compartments as well as the presence of BLB impairment [••29, ••30]. These methods are modifications of the grading system previously defined by Baráth et al., with the addition of mild (low-grade saccular) vestibular hydrops. The degree of vestibular hydrops is therefore classified on a 4-point scale (0: none; 1: mild hydrops; 2: moderate hydrops; 3: severe hydrops). Cochlear hydrops is categorized as none, grade 1 (moderate hydrops) or grade 2 (severe hydrops) [••29]. A detailed description of this classification system is provided in Table 3, and examples given in Figs. 2, 3 and 4.

Other MRI Features

The absence of hydrops or asymmetrical PE does not always classify the examination as "normal". Eliezer et al. reported non-visualization of the saccule (NVS) in a sub-group of MD patients [38]. The underlying mechanism has been hypothesized to be due to either collapse or fistula of the saccule, allowing a mixture of endolymph and (Gd-enhanced) perilymph, which has also been described on previous histopathologic studies in MD patients (Fig. 5) [78, 79]. It is of importance to realize that the endolymphatic spaces, particularly the saccule, represent very small anatomical structures. Care must be taken to ensure sufficient spatial resolution to prevent a false-positive diagnosis of saccular collapse or intralabyrinthine fistula, especially when bilateral NVS is observed. In addition, the afore-mentioned interaction between TI and the apparent size of the endolymphatic spaces should also be kept in mind. The distinction of the saccule and ampullae from the surrounding perilymph in healthy ears can be used as an indicator of the spatial resolution of the sequence.

Recently, Dubrulle et al. observed a nodular hyperintense signal in the region of the round window on delayed Gd-enhanced 3D-FLAIR MRI in 18 probable and definite MD patients. They hypothesized this "round window sign" to represent the presence of perilymphatic fistulae (not to be confused with intralabyrinthine fistulae), which was surgically confirmed in several of these patients. Knowledge of this entity is of importance, as perilymphatic fistulae are surgically correctable [80].

Table 3 Hydrops grading, according to van Steekelenburg et al. [29]

|	Grade	Details
Vestibule	1: Mild vestibular EH	The saccule is equal in size or larger than the utricle, but not confluent
	2: Moderate vestibular EH	Confluence of saccule and utricle that encompass > 50% of the vestibule
	3: Severe vestibular EH	Total effacement of the perilymphatic space in the vestibule
Cochlea	1: Moderate cochlear EH	Dilation of the scala media with partial obliteration of the scala vestibuli
	2: severe cochlear EH	Complete obliteration of the scala vestibuli
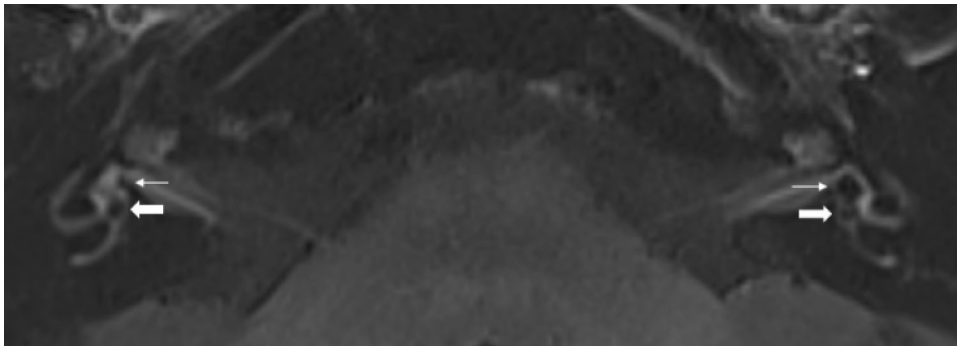
Fig. 2 Axial 4 h-delayed Gd-enhanced 3D-FLAIR MRI through the inferior part of the vestibule in a 53-year-old patient diagnosed with left-sided definite Menière's disease, according to the 2015 Bárány criteria. On the symptomatic side, the saccule (thin arrow) appears larger than the utricle (thick arrow), but not confluent, consistent with mild vestibular hydrops (low-grade saccular hydrops). Compare with a normal saccule on the right. There is no evidence of cochlear hydrops
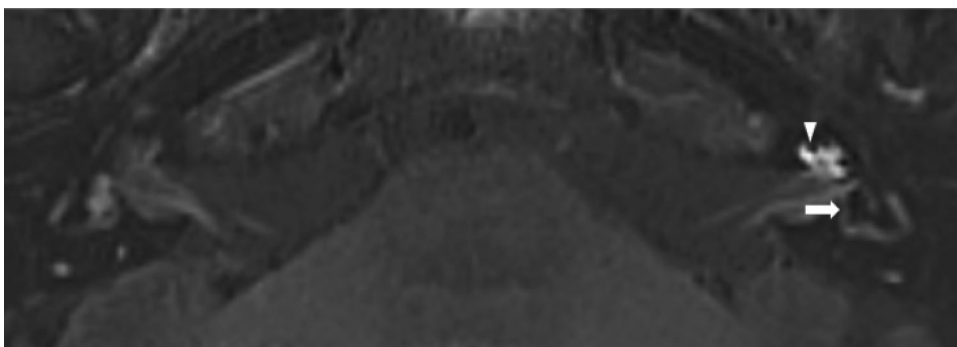

Fig. 3 Axial 4 h-delayed Gd-enhanced 3D-FLAIR MRI in a 58-year-old man with left-sided definite Menière's disease. The affected ear demonstrates moderate vestibular hydrops with confluence of the saccule and utricle that encompass > 50% of the vestibule (thick arrow). A thin rim of surrounding perilymph remains visible. In addition, there is moderate cochlear hydrops with partial effacement of the scala vestibuli (arrow head). Also note the increased perilymphatic enhancement in the symptomatic ear, which is believed to represent blood-labyrinth barrier impairment
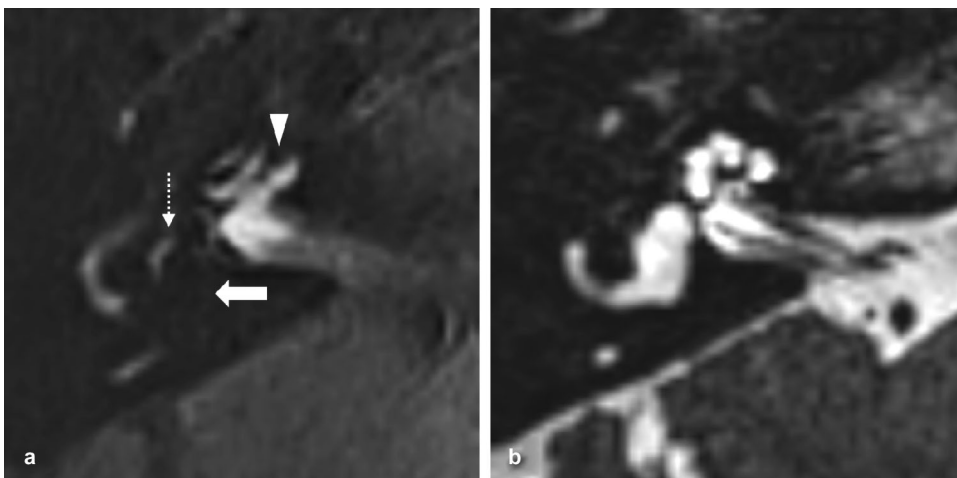

Fig. 4 Severe vestibular and cochlear hydrops in a 44-year-old man with unilateral definite Menière's disease. **a** Axial 4 h-delayed Gd-enhanced 3D-FLAIR MRI, showing severe vestibular hydrops with almost complete effacement of the surrounding perilymphatic space (thick arrow). Only a small rim of perilymph is visible at the base of the horizontal semicircular canal (dotted arrow). The scala vestibuli is completely obliterated by the enlarged cochlear duct indicating severe cochlear hydrops (arrowhead). This patient also demonstrated asymmetrical perilymphatic enhancement (contralateral ear not shown here). **b** Axial heavily T2-weighted sequence. Note that this sequence is particularly helpful for reference of the entire labyrinthine fluid space
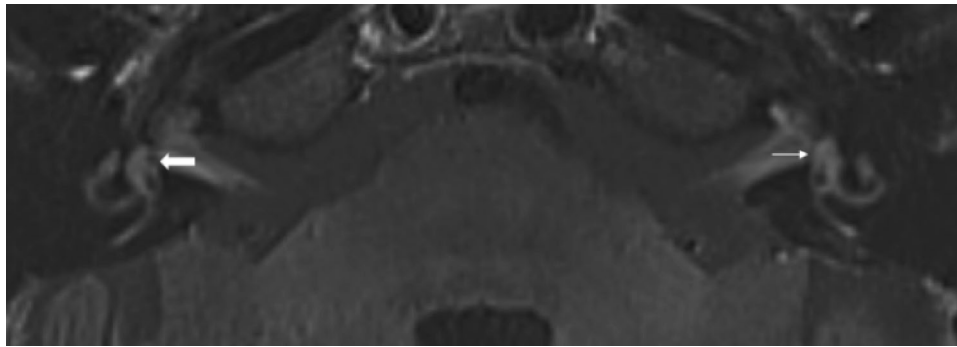
Fig. 5 Delayed post-contrast 3D-FLAIR MRI in a 73-year-old woman clinically diagnosed with left-sided definite Menière's disease. Non-visualization of the saccule on the left, suggestive of an intralabyrinthine fistula or collapse (thin arrow). Note the normal saccule in the unaffected right ear (thick arrow). In addition, the signal intensity of the perilymph is slightly increased in the left ear. There was no evidence of vestibular or cochlear hydrops

The possibility of evaluating the labyrinthine compartments in vivo has led to using hydrops sequences for other cochleovestibular diseases, such as idiopathic sudden sensorineural hearing loss, vestibular neuritis or vestibular areflexia [81–83]. Although these studies have yielded interesting results, a comprehensive discussion of the differential diagnosis of MD on hydrops MRI is beyond the scope of this review.

Clinical Application and Future Perspectives

It is important to distinguish MD from other vertigo-associated disorders in an early stage of the disease in order to provide proper counseling and optimize treatment strategies [84]. Delayed Gd-enhanced MRI has emerged as a reliable technique to demonstrate EH in patients suspected of MD in clinical practice. Especially the combination of vestibular hydrops and increased perilymph signal intensity in the affected ear due to BLB impairment is highly specific for MD [••29, ••30]. This is of particular relevance in patients in whom a formal MD diagnosis is hampered by atypical or non-specific symptoms, such as is the case in clinically suspected probable MD. It is likely that at least a proportion of individuals in this subthreshold category, based on current AAO-HNS criteria, actually have the same disorder as "true" MD but in insufficient degree to warrant a definite diagnosis on clinical grounds. The combination of EH and increased PE can be
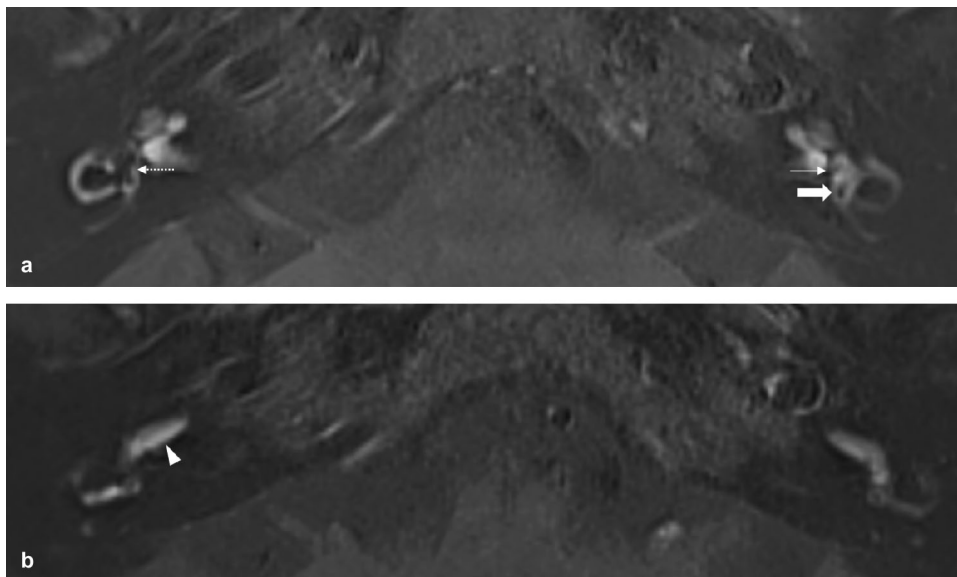

Fig. 6 A 62-year-old man diagnosed with right-sided probable Menière's disease, according to the 2015 Bárány criteria. **a** Axial delayed post-contrast 3D-FLAIR MRI centered at the pars inferior of the vestibule. The saccule and utricle in the right ear are confluent indicative of moderate vestibular hydrops (dotted arrow). Compare with a normal saccule (thin arrow) and utricle (thick arrow) in the contralateral ear. There is no evidence of cochlear hydrops. **b** The same patient, at the level of the basal cochlear turn. Note the increased perilymphatic enhancement in the symptomatic right ear, suggestive of BLB impairment (arrow head)

demonstrated in a substantial (43%) number of probable MD patients, which suggests a definite MD diagnosis in these individuals (Fig. 6) [••29]. However, clinical progression to the full-blown triad of MD in these individuals has yet to be confirmed by longitudinal studies.

MRI allows identification of the ear that is causing the vertigo in patients without concomitant auditory symptoms or other lateralizing signs on functional tests, which is relevant for targeted therapy [2]. The first line of care for MD patients comprises lifestyle adjustments, vestibular rehabilitation, psychotherapy, and medical treatment with betahistin or diuretics. If these therapies are to no avail, IT corticosteroids and surgical procedures can be considered. Ablative treatment with IT gentamycin is currently considered the most effective treatment for vertigo, but as a side effect carries a significant risk of hearing loss and vestibular hypofunction. [85, 86]. One could argue the benefit of delayed contrast enhanced MRI for clinically well-defined MD patients, as EH has been demonstrated in up to 96% of the affected ears in definite MD patients (2015 AAO-HNS criteria) [87]. However, EH has also been observed in contralateral asymptomatic MD ears in up to 65% of cases, which might be a preliminary sign of bilateral clinical disease [13, 88] (Fig. 7). Timely recognition of bilateral EH (in unilateral MD) may prompt counsel or treatment modification, and care must be taken with regard to ablative therapies of the symptomatic ear in these cases.

Currently, therapies for MD are evaluated clinically, based on natural history and/or audiovestibular tests [89].

Given the fluctuating nature of MD, differentiating between quiescent periods of the disease versus successful treatment can be difficult [•90]. Because MRI allows visualization of EH in vivo, this technique has potential as a surrogate marker of the disease to evaluate treatment response in individual patients and in treatment trials. Currently only a few reports on the visualization of EH after treatment have been published. Subsiding of EH has recently been described after oral acetazolamide, IT corticosteroids, and endolymphatic sac surgery [91–93]. However, Gürkov et al. found no effect of standard-dose oral betahistine on the degree of EH during a 7-month follow-up period [94]. Further research is needed to clarify the use and suitability of MRI for the evaluation of treatment response. Moreover, large-scale longitudinal studies are desirable to provide more insight in the dynamics of the hydropic process, with and without treatment, and how this relates to audiovestibular symptoms.

The above-mentioned indications illustrate the promising role of delayed contrast enhanced MRI, which may have important implications for future diagnostic criteria for MD. However, MRI methods and diagnostic imaging criteria for MD are still evolving and standardization is needed to fully implement MRI in clinical practice. In addition, an important prerequisite for the accurate diagnosis of EH is adequate quantification of the endolymphatic volume. Current grading systems mainly rely on visual and semi-quantitative assessment, but no definite objective tool for the assessment of EH currently exist. In addition, continued technological advances are expected to
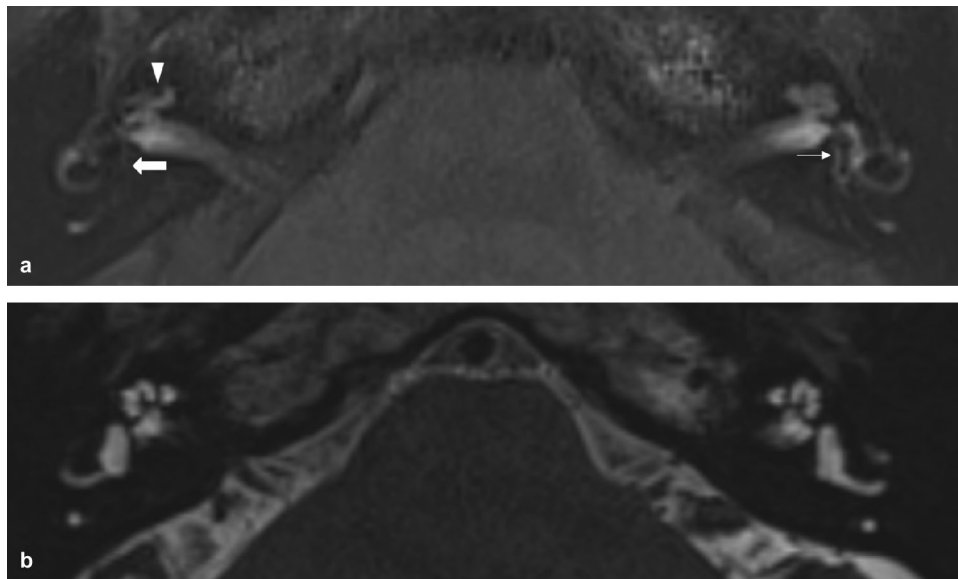

Fig. 7 Axial 4 h-delayed 3D-FLAIR MRI **a** and axial heavily T2-weighted sequence **b** in a 52-year-old woman with unilateral definite Menière's disease. In the symptomatic right ear, the thick arrow demonstrates severe vestibular hydrops with complete effacement of the surrounding perilymph. In addition, the scala media is enlarged with partial obliteration of the scala vestibuli consistent with moderate cochlear hydrops (arrow head). This patient had no left-sided auditory symptoms, but there is clear confluence of saccule and utricle in the left ear indicative of moderate vestibular hydrops. No cochlear hydrops was noted on this side

further improve spatial resolution and contrast on hydrops MRI. Current literature suggests that hydrops imaging may be feasible at 1.5 T after a single dose of IV GBCM; validation of this technique would permit broader application of delayed contrast enhanced inner ear MRI. It can be assumed that future studies will address these limitations.

Conclusions

In this review, we have summarized current MRI techniques for hydrops imaging and provided tools for clinical implementation. Detection of intralabyrinthine abnormalities in suspected MD patients can help establish the diagnosis, especially in ambiguous cases, and they have potential as a surrogate marker of disease for evaluating treatment response in individual patients and in treatment trials. Continued research is expected to further improve and validate MRI techniques for MD, particularly in the fields of image acquisition and interpretation.

Compliance with Ethical Guidelines

References

Recently published papers of particular interest have been highlighted as:
- Of importance
- •• Of major importance

1. Harcourt J, Barraclough K, Bronstein AM. Meniere's disease. BMJ. 2014;349:g6544.
2. Nakashima T, Pyykkö I, Arroll MA, Casselbrant ML, Foster CA, Manzoor NF, et al. Meniere's disease. Nat Rev Dis Prim [Internet]. 2016;2:16028. https://doi.org/10.1038/nrdp.2016.28.
3. Ménière P. Sur une forme de surdité grave dépendant d'une lésion de l'oreille interne. Gaz Méd Paris. 1861;1861(1629):16.
4. Atkinson M. Ménière's original papers reprinted with an English translation with commentaries and biographical sketch. Acta Otolaryngol. 1961;162:1–78.
5. House JW, Doherty JK, Fisher LM, Derebery MJ, Berliner KI. Meniere's disease: prevalence of contralateral ear involvement. Otol Neurotol. 2006;27:355.
6. Cairns H, Hallpike FRC. Observations on the pathology of Meniere's syndrome. J Laryngol Otol. 1938;31:1317.
7. Yamakawa K. Über die pathologische Veränderung bei einem Menière-Kranken. Proceedings of 42nd Annual Meeting Oto-Rhino-Laryngol Soc Japan. J Otolaryngol Soc Jpn. 1938;2310–2312.
8. Pender DJ. Endolymphatic hydrops and meniere's disease: a lesion meta-analysis. J Laryngol Otol. 2014;128:859–65.
9. •Oberman BS, Patel V A, Cureoglu S, Isildak H. The aetiopathologies of ménière's disease: a contemporary review. Acta Otorhinolaryngol Ital. 2017. *This review describes the current theories regarding the pathophysiology of Menière's disease.*
10. Committee on Hearing and Equilibrium guidelines for the diagnosis and evaluation of therapy in meniere's disease. American Academy of Otolaryngology-Head and Neck Foundation, Inc. Otolaryngol Head Neck Surg. 1995;113:181–5.
11. •Lopez-Escamez JA, Carey J, Chung WH, Goebel JA, Magnusson M, Mandalà M, et al. Diagnostic criteria for ménière's disease. J Vestib Res. 2015;25:1–7. *This consensus document of the Bárány Society, The Japan Society for Equilibrium Research, the European Academy of Otology and Neurotology (EAONO), the American Academy of Otolaryngology-Head and Neck Surgery (AAO-HNS) and the Korean Balance Society describes the latest clinical diagnostic criteria for Menière's disease.*
12. Goebel JA. 2015 Equilibrium committee amendment to the 1995 AAO-HNS guidelines for the definition of ménière's disease. Otolaryngol Head Neck Surg (United States). 2016;154:403–4.
13. Pyykkö I, Nakashima T, Yoshida T, Zou J, Naganawa S. Ménière's disease: a reappraisal supported by a variable latency of symptoms and the MRI visualisation of endolymphatic hydrops. BMJ Open [Internet]. 2013;3:1555. https://bmjopen.bmj.com
14. Nakashima T, Naganawa S, Sugiura M, Teranishi M, Sone M, Hayashi H, et al. Visualization of endolymphatic hydrops in patients with meniere's disease. Laryngoscope. 2007;117:415–20.
15. Nakashima T, Naganawa S, Teranishi M, Tagaya M, Nakata S, Sone M, et al. Endolymphatic hydrops revealed by intravenous gadolinium injection in patients with ménière's disease. Acta Otolaryngol. 2010;130:338–43.
16. Naganawa S, Nakashima T. Visualization of endolymphatic hydrops with MR imaging in patients with ménière's disease and related pathologies: current status of its methods and clinical significance. Jpn J Radiol. 2014;32:191–204.
17. Pyykkö I, Zou J, Poe D, Nakashima T, Naganawa S. Magnetic resonance imaging of the inner ear in meniere's disease. Otolaryngol Clin North Am. 2010;43:1059–80.
18. Lopez-Escamez JA, Attyé A. Systematic review of magnetic resonance imaging for diagnosis of meniere disease. J Vestib Res. 2019;29:121–9.

19. Zou J, Pyykkö I, Bretlau P, Klason T, Bjelke B. In vivo visualization of endolymphatic hydrops in guinea pigs: magnetic resonance imaging evaluation at 4.7 tesla. Ann Otol Rhinol Laryngol. 2003;112:1059–65.

20. Niyazov DM, Andrews JC, Strelioff D, Sinha S, Lufkin R. Diagnosis of endolymphatic hydrops in vivo with magnetic resonance Imaging. Otol Neurotol. 2001;22:813–7.

21. Shi H, Li Y, Yin S, Zou J. The predominant vestibular uptake of gadolinium through the oval window pathway is compromised by endolymphatic hydrops in ménière's disease. Otol Neurotol. 2014;35:315–22.

22. Nakashima T, Naganawa S, Katayama N, Teranishi M, Nakata S, Sugiura M, et al. Clinical significance of endolymphatic imaging after intratympanic gadolinium injection. Acta Otolaryngol. 2009;129:9–14.

23. Naganawa S, Yamazaki M, Kawai H, Bokura K, Sone M, Nakashima T. Visualization of endolymphatic hydrops in ménière's disease with single-dose intravenous gadolinium-based contrast media using heavily T(2)-weighted 3D-FLAIR. Magn Reson Med Sci. 2010;9:237.

24. ••Attyé A, Eliezer M, Boudiaf N, Tropres I, Chechin D, Schmerber S, et al. MRI of endolymphatic hydrops in patients with meniere's disease: a case-controlled study with a simplified classification based on saccular morphology. Eur Radiol. 2017;27:3138–46. *This paper describes the inversion of the saccule to utricle area ratio (SURI) as a criterion for the diagnosis of Menière's disease. In addition, non-visualization of the saccule, a novel MRI marker, which is thought to represent saccular collapse or an intralabyrinthine fistula, is described.*

25. Suzuki H, Teranishi M, Sone M, Yamazaki M, Naganawa S, Nakashima T. Contrast enhancement of the inner ear after intravenous administration of a standard or double dose of gadolinium contrast agents. Acta Otolaryngol. 2011;131:1025–31.

26. Naganawa S, Yamazaki M, Kawai H, Bokura K, Sone M, Nakashima T. Visualization of endolymphatic hydrops in ménière's disease after single-dose intravenous gadolinium-based contrast medium: timing of optimal enhancement. Magn Reson Med Sci. 2012;11:43–51.

27. Naganawa S, Suzuki K, Yamazaki M, Sakurai Y. Serial scans in healthy volunteers following intravenous administration of gadoteridol: time course of contrast enhancement in various cranial fluid spaces. Magn Reson Med Sci. 2014;13:7–13.

28. Naganawa S, Suzuki K, Yamazaki M, Sakurai Y, Ikeda M. Time course for measuring endolymphatic size in healthy volunteers following intravenous administration of Gadoteridol. Magn Reson Med Sci. 2014;13:73–80.

29. ••Steekelenburg JM van, Weijnen A van, de Pont LMH, Vijlbrief OD, Bommeljé CC, Koopman JP, et al. Value of endolymphatic hydrops and perilymph signal intensity in suspected ménière disease. Am J Neuroradiol. 2020;41:529–34. *This article describes the value of perilymphatic enhancement and endolymphatic hydrops in discriminating between Menière's disease and other vertigo-associated inner ear disorders. In addition, a four grade grading system for endolymphatic hydrops and cochlear perilymphatic enhancement is described.*

30. ••Bernaerts A, Vanspauwen R, Blaivie C, van Dinther J, Zarowski A, Wuyts FL, et al. The value of four stage vestibular hydrops grading and asymmetric perilymphatic enhancement in the diagnosis of ménière's disease on MRI. Neuroradiology. 2019;61:421–9. *This article describes a four-stage grading system for endolymphatic hydrops in combination with cochlear perilymphatic enhancement.*

31. Pai I, Mendis S, Murdin L, Touska P, Connor S. Magnetic resonance imaging of Ménière' s disease: early clinical experience in a UK centre. J Laryngol Otol. 2020;134:302–10.

32. Zhang W, Hui L, Zhang B, Ren L, Zhu J, Wang F, et al. The correlation between endolymphatic hydrops and clinical features of meniere disease. Laryngoscope. 2020. https://doi.org/10.1002/lary.28576.

33. Yamazaki M, Naganawa S, Tagaya M, Kawai H, Ikeda M, Sone M, et al. Comparison of contrast effect on the cochlear perilymph after intratympanic and intravenous gadolinium injection. Am J Neuroradiol. 2012;33:773–8.

34. Louza J, Krause E, Gürkov R. Audiologic evaluation of ménière's disease patients one day and one week after intratympanic application of gadolinium contrast agent: our experience in sixty-five patients. Clin Otolaryngol. 2013;38:262–6.

35. Louza JPR, Flatz W, Krause E, Gürkov R. Short-term audiologic effect of intratympanic gadolinium contrast agent application in patients with ménière's disease. Am J Otolaryngol Head Neck Med Surg [Internet]. 2012;33:533–7. https://doi.org/10.1016/j.amjoto.2011.12.004.

36. Louza J, Krause E, Gürkov R. Hearing function after intratympanic application of gadolinium-based contrast agent: a long-term evaluation. Laryngoscope. 2015;125:2366–70.

37. •Loureiro RM, Sumi DV, Tames HL de VC, Soares CR, Salmito MC, Gomes RLE, et al. Endolymphatic hydrops evaluation on MRI: practical considerations. Am J Otolaryngol Head Neck Med Surg [Internet]. 2020;41:102361. https://doi.org/10.1016/j.amjoto.2019.102361. *This paper describes practical considerations for hydrops imaging.*

38. Eliezer M, Poillon G, Lévy D, Guichard J, Houdart E, Attyé A, et al. Clinical and radiological characteristics of patients with collapse or fistula of the saccule as evaluated by inner ear MRI. Acta Otolaryngol [Internet]. Taylor & Francis; 2020;140:262–9. https://doi.org/10.1080/00016489.2020.1713396

39. Gürkov R, Jerin C, Flatz W, Maxwell R. Clinical manifestations of hydropic ear disease (Ménière's). Eur Arch Oto-Rhino-Laryngol. 2019;276:27–40.

40. Suzuki H, Teranishi M, Naganawa S, Nakata S, Sone M, Nakashima T. Contrast-enhanced MRI of the inner ear after intratympanic injection of meglumine gadopentetate or gadodiamide hydrate. Acta Otolaryngol. 2011;131:130–5.

41. Eliezer M, Poillon G, Gillibert A, Horion J, Cruypeninck Y, Gerardin E, et al. Comparison of enhancement of the vestibular perilymph between gadoterate meglumine and gadobutrol at 3-Tesla in meniere's disease. Diagn Interv Imaging [Internet]. 2018;99:271–7. https://doi.org/10.1016/j.diii.2018.01.002.

42. Kanal E, Maravilla K, Rowley HA. Gadolinium contrast agents for CNS imaging: current concepts and clinical evidence. Am J Neuroradiol. 2014;35:2215–26.

43. Naganawa S. The technical and clinical features of 3D-FLAIR in neuroimaging. Magn Reson Med Sci. 2015;14:93–106.

44. Park HW, Cho MH, Cho ZH. Real-value representation in inversion-recovery NMR imaging by use of a phase-correction method. Magn Reson Med. 1986;3:15–23.

45. Nakashima T, Naganawa S, Pyykkö I, Gibson WPR, Sone M, Nakata S, et al. Grading of endolymphatic hydrops using magnetic resonance imaging. Acta Otolaryngol. 2009. https://doi.org/10.1080/00016480902729827.

46. Naganawa S, Satake H, Kawamura M, Fukatsu H, Sone M, Nakashima T. Separate visualization of endolymphatic space, perilymphatic space and bone by a single pulse sequence; 3D-inversion recovery imaging utilizing real reconstruction after intratympanic Gd-DTPA administration at 3 Tesla. Eur Radiol. 2008;18:920–4.

47. •Eliezer M, Gillibert A, Tropres I, Krainik A, Attyé A. Influence of inversion time on endolymphatic hydrops evaluation in 3D-FLAIR imaging. J Neuroradiol [Internet]. Elsevier Masson SAS; 2017;44:339–43. https://doi.org/10.1016/j.neurad.2017.06.002.

This paper describes the relation between Inversion Time (TI) and the endolymph-perilymph ratio at delayed Gd-enhanced 3D-FLAIR MRI at 3T. In addition, the role of the saccule in the analysis of Menière's disease is discussed.

48. Grieve SM, Obholzer R, Malitz N, Gibson WP, Parker GD. Imaging of endolymphatic hydrops in meniere's disease at 1.5 T using phase-sensitive inversion recovery: (1) demonstration of feasibility and (2) overcoming the limitations of variable gadolinium absorption. Eur J Radiol. 2012;81:331–8.

49. Bykowski J, Harris JP, Miller M, Du J, Mafee MF. Intratympanic contrast in the evaluation of menière disease: understanding the limits. Am J Neuroradiol. 2015;36:1326–32.

50. Naganawa S, Kawai H, Sone M, Nakashima T. Increased sensitivity to low concentration gadolinium contrast by optimized heavily T2-weighted 3D-FLAIR to visualize endolymphatic space. Magn Reson Med Sci. 2010;9:73–80.

51. Naganawa S, Kawai H, Taoka T, Sone M. Improved HYDROPS: imaging of endolymphatic hydrops after intravenous administration of gadolinium. Magn Reson Med Sci. 2017;16:357–61.

52. Attyé A, Dumas G, Troprès I, Roustit M, Karkas A, Banciu E, et al. Recurrent peripheral vestibulopathy: is MRI useful for the diagnosis of endolymphatic hydrops in clinical practice? Eur Radiol. 2015;25:3043–9.

53. Venkatasamy A, Veillon F, Fleury A, Eliezer M, Abu Eid M, Romain B, et al. Imaging of the saccule for the diagnosis of endolymphatic hydrops in meniere disease, using a three-dimensional T2-weighted steady state free precession sequence: accurate, fast, and without contrast material intravenous injection. Eur Radiol Exp. 2017;1:14.

54. Simon F, Guichard JP, Kania R, Franc J, Herman P, Hautefort C. Saccular measurements in routine MRI can predict hydrops in menière's disease. Eur Arch Oto-Rhino-Laryngol. 2017;274:4113–200.

55. •Nahmani S, Vaussy A, Hautefort C, Guichard J-P, Guillonnet A, Houdart E, et al. Comparison of enhancement of the vestibular perilymph between variable and constant flip angle—delayed 3D-FLAIR sequences in menière disease. Am J Neuroradiol. 2020;41:706–11. *This paper compares the post-contrast signal intensity of the perilymph between a constant flip angle 3D-FLAIR sequence and a heavily T2-weighted variable flip angle sequence respectively.*

56. Baráth K, Schuknecht B, Monge Naldi A, Schrepfer T, Bockisch CJ, Hegemann SCA. Detection and grading of endolymphatic hydrops in menière disease using MR imaging. Am J Neuroradiol. 2014;35:1387–92.

57. Lane JI, Witte RJ, Bolster B, Bernstein MA, Johnson K, Morris J. State of the art: 3T imaging of the membranous labyrinth. Am J Neuroradiol. 2008;29:1436–40.

58. Naganawa S, Suzuki K, Nakamichi R, Bokura K, Yoshida T, Sone M, et al. Semi-quantification of endolymphatic size on MR imaging after intravenous injection of single-dose gadodiamide: comparison between two types of processing strategies. Magn Reson Med Sci. 2013;12:261–9.

59. Attyé A, Barma M, Schmerber S, Dumas G, Eliezer M, Krainik A. The vestibular aqueduct sign: magnetic resonance imaging can detect abnormalities in both ears of patients with unilateral meniere's disease. J Neuroradiol [Internet]. 2020;47:174–9. https://doi.org/10.1016/j.neurad.2018.10.003.

60. Naganawa S, Yamazaki M, Kawai H, Sone M, Nakashima T. Contrast enhancement of the anterior eye segment and infarachnoid space: detection in the normal state by heavily T 2-weighted 3D FLAIR. Magn Reson Med Sci. 2011;10:193–9.

61. Fang ZM, Chen X, Gu X, Liu Y, Zhang R, Cao DR, et al. A new magnetic resonance imaging scoring system for perilymphatic space appearance after intratympanic gadolinium injection, and its clinical application. J Laryngol Otol. 2012;126:454–9.

62. Kahn L, Hautefort C, Guichard JP, Toupet M, Jourdaine C, Vitaux H, et al. Relationship between video head impulse test, ocular and cervical vestibular evoked myogenic potentials, and compartmental magnetic resonance imaging classification in menière's disease. Laryngoscope. 2019;130:1–9.

63. Shi S, Zhou F, Wang W. 3D-real IR MRI of meniere's disease with partial endolymphatic hydrops. Am J Otolaryngol Head Neck Med Surg [Internet]. 2019;40:589–93. https://doi.org/10.1016/j.amjoto.2019.05.015.

64. Fiorino F, Pizzini FB, Beltramello A, Barbieri F. Progression of endolymphatic hydrops in meniere's disease as evaluated by magnetic resonance imaging. Otol Neurotol. 2011;32:1152–7.

65. Gürkov R. Menière and friends: imaging and classification of hydropic ear disease. Otol Neurotol. 2017;38:e539–e544544.

66. Salt AN, Plontke SK. Endolymphatic hydrops: pathophysiology and experimental models. Otolaryngol Clin North Am. 2010;43:971–83.

67. Naganawa S, Kawai H, Sone M, Nakashima T, Ikeda M. Endolympathic hydrops in patients with vestibular schwannoma: visualization by non-contrast-enhanced 3D FLAIR. Neuroradiology. 2011;53:1009–155.

68. Wang F, Yoshida T, Sugimoto S, Shimono M, Teranishi M, Naganawa S, et al. Clinical features of ears with otosclerosis and endolymphatic hydrops. Otol Neurotol. 2019;40:441–5.

69. Butman JA, Nduom E, Kim HJ, Lonser RR. Imaging detection of endolymphatic sac tumor-associated hydrops. J Neurosurg. 2013;119:406–11.

70. ••Gürkov R, Hornibrook J. On the classification of hydropic ear disease (Menière's disease). HNO. 2018;66:455–63. *This article reviews and discusses classification proposals for Menière's disease, including the recent classification system of hydropic ear disease.*

71. Tagaya M, Yamazaki M, Teranishi M, Naganawa S, Yoshida T, Otake H, et al. Endolymphatic hydrops and blood-labyrinth barrier in meniere's disease. Acta Otolaryngol. 2011;131:474–9.

72. Pakdaman MN, Ishiyama G, Ishiyama A, Peng KA, Kim HJ, Pope WB, et al. Blood-labyrinth barrier permeability in menière disease and idiopathic sudden sensorineural hearing loss: findings on delayed postcontrast 3D-FLAIR MRI. Am J Neuroradiol. 2016;37:1903–8.

73. Ishiyama G, Lopez IA, Ishiyama P, Vinters HV, Ishiyama A. The blood labyrinthine barrier in the human normal and meniere's disease macula utricle. Sci Rep. 2017;7:253.

74. Eliezer M, Horion J, Magne N, Maquet C, Bolognini B, Gillibert A, et al. Detection of intralabyrinthine abnormalities using postcontrast delayed 3D-FLAIR MRI sequences in patients with acute vestibular syndrome. Eur Radiol. 2019;29:2760–9.

75. Kim T, Park D, Lee Y, Lee S, Chung J, Lee S. Comparisons of contrast enhancement on inner ear among patients with unilateral otologic symptoms in 3D flair MR images at 10 minutes and 4 hour after gadolinium injection. Neuroradiology [Internet]. 2015;36:2367–72. https://www.embase.com/search/results?subaction=viewrecord&from=export&id=L71812890%0Ahttps://sfx.library.uu.nl/utrecht?sid=EMBASE&issn=00283940&id=doi:&atitle=Comparisons+of+contrast+enhancement+on+inner+ear+among+patients+with+unilateral+otologic+symptoms

76. Lammers MJW, Young E, Fenton D, Lea J, Westerberg BD. The prognostic value and pathophysiologic significance of three-dimensional fluid-attenuated inversion recovery (3D-FLAIR) magnetic resonance imaging in idiopathic sudden sensorineural hearing loss: a systematic review and meta-analysis. Clin Otolaryngol. 2019;44:1017–25.

77. Yamazaki M, Naganawa S, Kawai H, Nihashi T, Fukatsu H, Nakashima T. Increased signal intensity of the cochlea on pre- and post-contrast enhanced 3D-FLAIR in patients with vestibular schwannoma. Neuroradiology. 2009;51:855–63.

78. Kimura RS, Schuknecht HF. Effect of fistulae on endolymphatic hydrops. Ann Otol Rhinol Laryngol. 1975;84:271–86.

79. Kitamura K, Schuknecht HF, Kimura RS. Cochlear hydrops in association with collapsed saccule and ductus reuniens. Ann Otol Rhinol Laryngol. 1982;91:5–13.

80. Dubrulle F, Chaton V, Risoud M, Farah H, Charley Q, Vincent C. The round window sign: a sensitive sign to detect perilymphatic fistulae on delayed postcontrast 3D-FLAIR sequence. Eur Radiol. 2020. https://doi.org/10.1007/s00330-020-06924-4.

81. Lee JI, Yoon RG, Lee JH, Park JW, Yoo MH, Ahn JH, et al. Prognostic value of labyrinthine 3D-FLAIR abnormalities in idiopathic sudden sensorineural hearing loss. Am J Neuroradiol. 2016;37:2317–22.

82. Byun H, Chung JH, Lee SH, Park CW, Park DW, Kim TY. Clinical value of 4-hour delayed gadolinium-enhanced 3D FLAIR MR images in acute vestibular neuritis. Laryngoscope. 2018;128:1946–51.

83. Attyé A, Eliezer M. Endolymph magnetic resonance imaging: contribution of saccule and utricle analysis in the management of patients with sensorineural ear disorders. Eur Ann Otorhinolaryngol Head Neck Dis [Internet]. 2020;137:47–51. https://doi.org/10.1016/j.anorl.2019.11.001.

84. Sharon JD, Trevino C, Schubert MC, Carey JP. Treatment of menière's disease. Curr Treat Options Neurol. 2015;17:341.

85. Nevoux J, Barbara M, Dornhoffer J, Gibson W, Kitahara T, Darrouzet V. International consensus (ICON) on treatment of meniere's disease. Eur Ann Otorhinolaryngol Head Neck Dis. 2018;135:S29–32.

86. Sharon JD, Trevino C, Schubert MC, Carey JP. Treatment of ménière's disease. Curr Treat Options Neurol. 2015;17:341.

87. Shi S, Guo P, Wang W. Magnetic resonance imaging of ménière's disease after intravenous administration of gadolinium. Ann Otol Rhinol Laryngol. 2018;127:777–82.

88. Wu Q, Dai C, Zhao M, Sha Y. The correlation between symptoms of definite meniere's disease and endolymphatic hydrops visualized by magnetic resonance imaging. Laryngoscope. 2016;126:974–9.

89. Tassinari M, Mandrioli D, Gaggioli N, di Sarsina RP. Ménière's disease treatment: a patient-centered systematic review. Audiol Neurotol. 2015;20:153–65.

90. •Basura GJ, Adams ME, Monfared A, Schwartz SR, Antonelli PJ, Burkard R, et al. Clinical practice guideline: ménière's disease. Otolaryngol Head Neck Surg (United States). 2020;162:S1–55. *This clinical practice guideline summarizes the latest scientific and clinical evidence regarding the diagnostic workup and treatment of Menière's disease.*

91. Landen M, Bernaerts A, Vanspauwen R, Deckers F, De FB. Downgrading of endolymphatic hydrops on MRI after intratympanic corticosteroid therapy in a patient with menière's disease. Otol Neurotol. 2020;41:e638–e640640.

92. Ito T, Inui H, Miyasaka T, Shiozaki T, Matsuyama S, Yamanaka T, et al. Three-dimensional magnetic resonance imaging reveals the relationship between the control of vertigo and decreases in endolymphatic hydrops after endolymphatic sac drainage with steroids for meniere's disease. Front Neurol. 2019;4:46.

93. Sepahdari A, Vorasubin N, Ishiyama G, Ishiyama A. Endolymphatic hydrops reversal following acetazolamide therapy: demonstration with delayed intravenous contrast-enhanced 3D-FLAIR MRI. Am J Neuroradiol. 2016;37:151–4.

94. Gürkov R, Flatz W, Keeser D, Strupp M, Ertl-Wagner B, Krause E. Effect of standard-dose betahistine on endolymphatic hydrops: an MRI pilot study. Eur Arch Oto-Rhino-Laryngol. 2013;270:1231–5.

95. Gürkov R, Flatz W, Louza J, Strupp M, Krause E. In vivo visualization of endolyphatic hydrops in patients with meniere's disease: correlation with audiovestibular function. Eur Arch Oto-Rhino-Laryngology. 2011;268:1743.